

Chapter 29

Raman Spectroscopy of Vanadium Oxide Supported on Alumina

G. Deo¹, F. D. Hardcastle¹, M. Richards¹, A. M. Hirt²,
and Israel E. Wachs¹

¹Departments of Chemistry and Chemical Engineering, Zettlemoyer Center
for Surface Studies, Lehigh University, Bethlehem, PA 18015

²Materials Research Laboratories, Inc., 720 King Georges Post Road,
Fords, NJ 08863

The molecular state of vanadium oxide supported on different alumina phases (γ , δ - θ , and α) was investigated with Raman spectroscopy. The supported vanadium oxide was found to form a molecularly dispersed overlayer on the different alumina phases. The molecular state of the surface vanadium oxide phase, however, was dependent on the nature of the alumina support. This variation was primarily due to the presence of surface impurities, in particular sodium oxide. The surface sodium oxide content was found to increase with the calcination temperature required to form the different transitional alumina phases (α , δ - θ , γ). The surface vanadium oxide phase consists of polymeric tetrahedra and distorted octahedra on γ -Al₂O₃, monomeric tetrahedra and distorted octahedra on δ , θ -Al₂O₃, and monomeric tetrahedra on α -Al₂O₃.

Recent studies of supported vanadium oxide catalysts have revealed that the vanadium oxide component is present as a two-dimensional metal oxide overlayer on oxide supports (1). These surface vanadium oxide species are more selective than bulk, crystalline V₂O₅ for the partial oxidation of hydrocarbons (2). The molecular structures of the surface vanadium oxide species, however, have not been resolved (1,3,4). A characterization technique that has provided important information and insight into the molecular structures of surface metal oxide species is Raman spectroscopy (2,5). The molecular structures of metal oxides can be determined from Raman spectroscopy through the use of group theory, polarization data, and comparison of the

0097-6156/90/0437-0317\$06.00/0

© 1990 American Chemical Society

Raman spectra with spectra of known molecular structures (6).

In the present investigation, the interaction of vanadium oxide with different alumina phases (γ , δ - θ , and α) is examined with Raman spectroscopy. Comparison of the Raman spectra of the supported vanadium oxide catalysts with those obtained from vanadium oxide reference compounds allows for the structural assignment of these supported species. The present Raman data demonstrate that the molecular structures of the surface vanadium oxide phases are significantly influenced by the presence of surface impurities on the alumina supports and this overshadows the influence, if any, of the alumina substrate phase.

EXPERIMENTAL

The γ phase (Harshaw, 180m²/gm), δ , θ phase (Harshaw, 120m²/gm), and α phase (ALCOA, 9.5m²/gm) of Al₂O₃ were used in this study. δ , θ -Al₂O₃ was prepared by heating the starting γ -Al₂O₃ at 950°C in O₂. X-ray diffraction was used to confirm the presence of the respective alumina phases. The vanadium oxide catalysts were prepared by incipient-wetness impregnation of vanadium triisopropoxide (Alfa) using methanol as the solvent. Due to the air and moisture sensitive nature of the alkoxide precursor, the catalysts were prepared and subsequently heated in N₂ at 350°C. The catalysts were finally calcined in O₂ at 500°C for 16 hrs. All samples are noted as weight percent V₂O₅/Al₂O₃. Surface areas were measured with a Quantachrome BET apparatus using single point nitrogen adsorption. The arrangement of the laser Raman spectrometer has been described elsewhere (5,7). Surface impurities on different alumina phases were measured on a Model DS800 XPS surface analysis system manufactured by KRATOS Analytical Plc, Manchester UK. Specimens were prepared by pressing the different alumina phases between a stainless steel holder and a polished single crystal silicon wafer. Measurements were done at 5.10⁻⁹ Torr with an hemispherical electron energy analyzer used for electron detection. Mg-K α x-rays at a power of 360 W were employed in this study and the data were collected in 0.75 eV segments for a total of 1 hour. A pass energy of 80 eV was used for each of the specimens. The electron spectrometer was operated in the fixed analyzer transmission (FAT) mode. Elemental identification from each spectrum were done by comparing the measured peak energy to tabulated values and concentration estimates were made using typical normalization procedures (8).

RESULTS AND DISCUSSION

The major vibrational region of interest in the Raman spectra of vanadium(V) oxide structures lies in the

1200-100 cm^{-1} range. For vanadium oxide systems this region can be primarily divided into three parts. The V-O terminal stretching which occurs at 770-1050 cm^{-1} , the V-O-V stretching region at 500-800 cm^{-1} , and the bending mode at 150-400 cm^{-1} . Lattice vibrations of crystalline compounds may be also present below 150 cm^{-1} .

Vanadium(V) Oxide Reference Compounds

It is known that under ambient conditions supported vanadium oxide exists as a +5 cation (9). For this reason the Raman spectra of some pentavalent vanadium oxide reference compounds were studied. The vanadium(V) oxide reference compounds can be primarily categorized as tetrahedral or octahedral compounds. The structures of these reference compounds have been previously determined and only a brief discussion will be given here. Raman spectra of the vanadium(V) oxide reference compounds are shown in Figures 1-2.

Spectra of tetrahedral vanadium(V) oxide compounds are shown in Figure 1 with different degrees of polymerization of the monomeric VO_4 unit. The Raman band associated with the terminal V-O bond increases with increasing extent of polymerization : ~ 830 cm^{-1} for monomeric VO_4^{3-} , ~ 880 cm^{-1} for dimeric $\text{V}_2\text{O}_7^{4-}$, and ~ 940 cm^{-1} for a chain composed of VO_4 units. Due to the presence of V-O-V linkages in the dimeric and polymeric species the bond length of the bridging bonds increase which gives rise to a higher order of the terminal V-O bonds and consequently a higher frequency. The monomeric unit in $\text{Pb}_5(\text{VO}_4)_3\text{Cl}$ gives rise to Raman bands at ~ 830 cm^{-1} (symmetric stretch), ~ 790 cm^{-1} (antisymmetric stretch), and bending modes at 320-350 cm^{-1} . Distortions imposed on the VO_4^{3-} unit will also increase the bond order and shift the Raman band to higher frequencies. For example, AlVO_4 possesses three different, highly distorted monomeric VO_4^{3-} units, and the corresponding Raman spectrum exhibits a triplet in the 980-1020 cm^{-1} region. The presence of V-O-V linkages is readily identified with Raman spectroscopy since they give rise to new modes at 200-300 cm^{-1} (bending), and 400-500 cm^{-1} (symmetric stretch), and 600-800 cm^{-1} (antisymmetric stretch). The Raman spectra of tetrahedral vanadium oxide species in aqueous solution also have similar features (6).

Spectra of octahedral vanadium(V) oxide compounds are presented in Figure 2. Undistorted vanadium(V) oxide compounds do not exist, and all vanadia octahedra are highly distorted, which give rise to short V-O bonds. This is reflected in the Raman band position for the distorted octahedral vanadium oxide compounds which always occur in the 900-1000 cm^{-1} region. The vanadia structure in V_2O_5 approaches a square-pyramidal coordination and the individual vanadia are linked

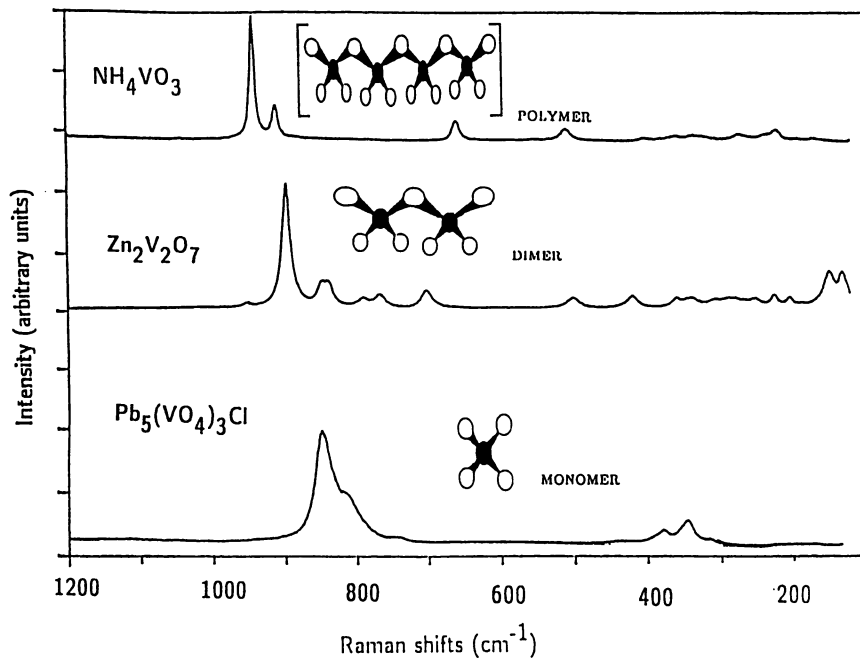


FIGURE 1. Raman Spectra of Tetrahedral Vanadium(V) Oxide Reference Compounds.

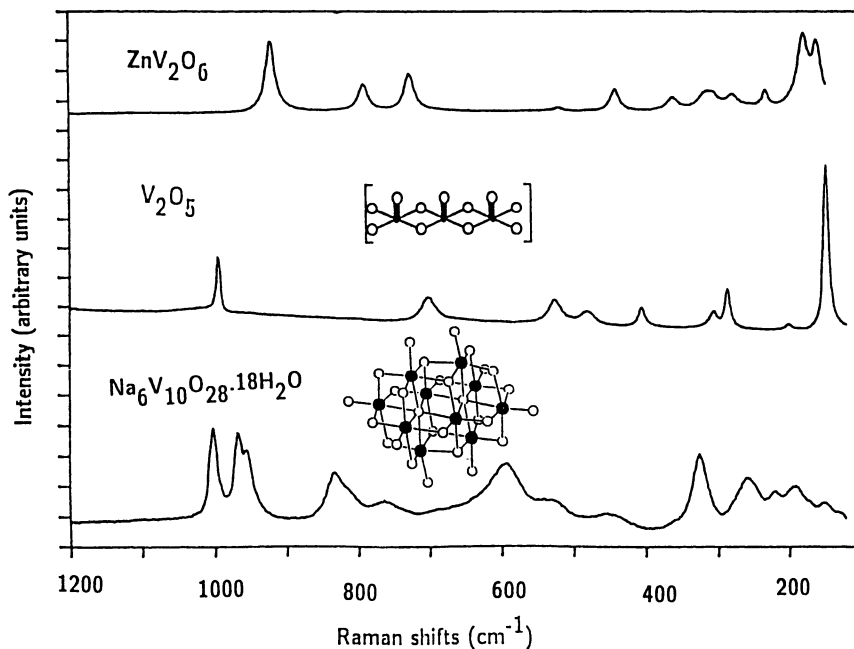


FIGURE 2. Raman Spectra of Octahedral Vanadium(V) Oxide Reference Compounds.

together to form infinite sheets (10). The short V-O bond in this structure is responsible for the band at 997 cm^{-1} (10). Many bands in the 200-800 region are due to the V-O-V linkages, and the strong band at $\sim 144\text{ cm}^{-1}$ arises from the lattice vibrations (11). The decavanadate ion in $\text{Na}_6\text{V}_{10}\text{O}_{28}\cdot 18\text{H}_2\text{O}$ is made up of three distinctly different and distorted vanadia octahedra (12). Two of the vanadia octahedra approach a square-pyramidal coordination and the third has two short bonds cis to each other. The presence of three types of terminal V-O bonds in the decavanadate ion can be seen from the Raman spectra which give rise to strong bands at ~ 1000 , 966 and 954 cm^{-1} . Due to the presence of numerous V-O-V linkages in the decavanadate structure, a number of strong Raman bands in the V-O-V bending ($150\text{-}300\text{ cm}^{-1}$) and V-O-V stretching ($500\text{-}800\text{ cm}^{-1}$) regions are present. The vanadia octahedral ion present in ZnV_2O_6 is not as distorted as those found in V_2O_5 and $\text{Na}_6\text{V}_{10}\text{O}_{28}\cdot 18\text{H}_2\text{O}$ and consequently exhibits a strong stretching band at $910\text{-}920\text{ cm}^{-1}$ (13). Numerous V-O-V associated bands are also present in the $150\text{-}800\text{ cm}^{-1}$ region.

The Alumina Supports

The Raman spectra of γ , δ,θ , and $\alpha\text{-Al}_2\text{O}_3$ are shown in Figure 3. For $\gamma\text{-Al}_2\text{O}_3$ there are no Raman bands in the $150\text{-}1200\text{ cm}^{-1}$ region. For $\delta,\theta\text{-Al}_2\text{O}_3$ several Raman bands are observed: two bands of medium intensity at ~ 837 and $\sim 753\text{ cm}^{-1}$, and a strong band at $\sim 251\text{ cm}^{-1}$. The α phase of Al_2O_3 possesses Raman bands at 742, 631, 577, 416, and 378 cm^{-1} . The surface compositions of the alumina supports were determined by X-ray Photoelectron Spectroscopy and are shown in Table I. In addition to the impurities present on $\gamma\text{-Al}_2\text{O}_3$, δ,θ and $\alpha\text{-Al}_2\text{O}_3$ show the presence of sodium and fluorine ions. These impurities may result from the manufacturing process (e.g. Bayer process) or incomplete purification of the ore (14).

$\text{V}_2\text{O}_5/\text{Al}_2\text{O}_3$

The supported vanadium oxide on $\gamma\text{-Al}_2\text{O}_3$ is present as a well dispersed phase for 3-20% $\text{V}_2\text{O}_5/\text{Al}_2\text{O}_3$ (Figure 4). The Raman spectra of $\text{V}_2\text{O}_5/\gamma\text{-Al}_2\text{O}_3$ have been discussed before (11), and the vanadium oxide structure has been classified into three main regions. Above 20% $\text{V}_2\text{O}_5/\text{Al}_2\text{O}_3$, the Raman spectra show the formation of V_2O_5 crystallites. At 5% $\text{V}_2\text{O}_5/\text{Al}_2\text{O}_3$ and below, the Raman band is present at $\sim 940\text{ cm}^{-1}$ which is typical of the terminal stretching mode found in alkali metavanadates which possess polymeric chains of VO_4 units (Figure 1). The corresponding V-O-V vibrations of metavanadates are also present in these samples. Above 5% $\text{V}_2\text{O}_5/\text{Al}_2\text{O}_3$, new bands

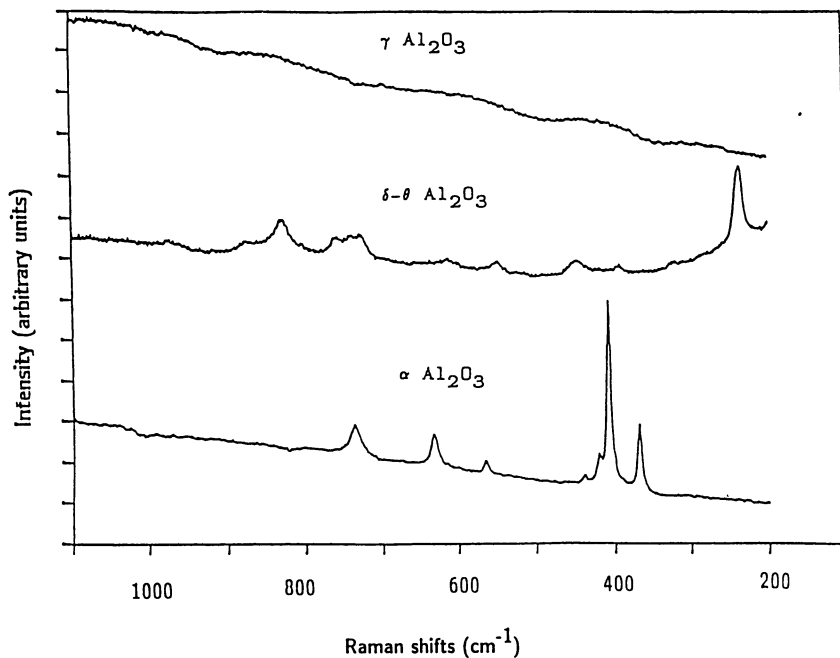


FIGURE 3. Raman Spectra of Alumina Supports.

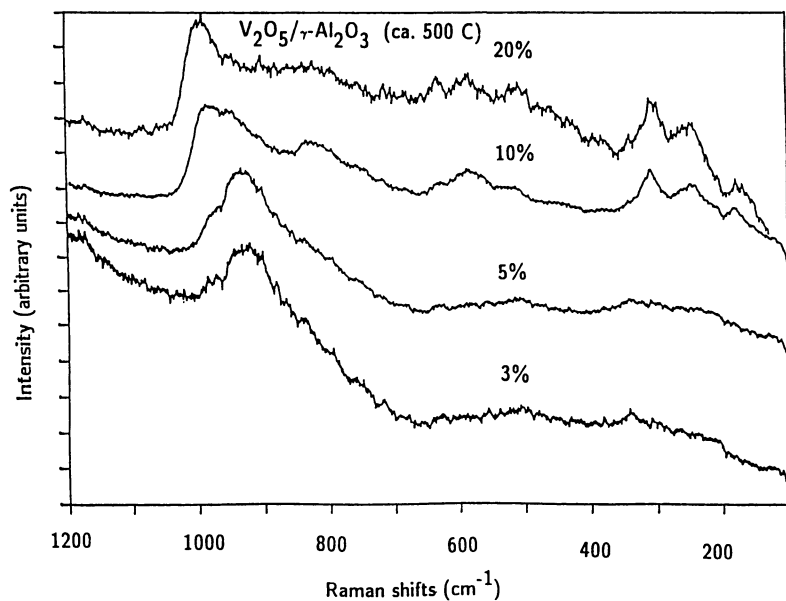


FIGURE 4. Raman Spectra of Vanadium Oxide Supported on γ - Al_2O_3 .

Table I. Surface concentrations on different alumina supports (in atomic %)

Surface Atom	Alumina Support Phase		
	α	δ, θ	γ
C	5.5	4.7	7.5
O	57.1	59.6	58.2
F	0.27	0.28	----
Na	0.98	0.18	----
Al	35.5	34.9	33.5
Cl	0.6	0.4	0.86

appear near the 1000 cm^{-1} region which are due to a vanadium oxygen double bond and are associated with the highly distorted octahedral environment of the vanadium oxide species (Figure 2). Solid state ^{51}V NMR studies of these samples confirm that tetrahedral surface vanadia species are exclusively formed in the 0-5% $\text{V}_2\text{O}_5/\gamma\text{-Al}_2\text{O}_3$ range and that distorted octahedral surface species are predominately present above 5% $\text{V}_2\text{O}_5/\gamma\text{-Al}_2\text{O}_3$ (4). The 10% $\text{V}_2\text{O}_5/\gamma\text{-Al}_2\text{O}_3$ also has broad bands at 950-1000, at 810-830, 550-580, ~ 500, 290-300, ~ 250, and ~ 180 cm^{-1} . There is a striking similarity between the position of these Raman bands and the Raman bands found in $\text{Na}_6\text{V}_{10}\text{O}_{28}\cdot 18\text{H}_2\text{O}$ (Figure 2). Similar Raman bands are also present for 20% $\text{V}_2\text{O}_5/\gamma\text{-Al}_2\text{O}_3$. Thus, the supported vanadium oxide phase seems to be present with units similar to the decavanadate ion in 10-20% $\text{V}_2\text{O}_5/\gamma\text{-Al}_2\text{O}_3$.

The Raman spectra for 1-10% $\text{V}_2\text{O}_5/\delta, \theta\text{-Al}_2\text{O}_3$ are shown in Figure 5. Crystalline bands appear at 13% $\text{V}_2\text{O}_5/\delta, \theta\text{-Al}_2\text{O}_3$ indicating that monolayer coverage of surface vanadium oxide has been exceeded. 1-5% $\text{V}_2\text{O}_5/\delta, \theta\text{-Al}_2\text{O}_3$ samples possess Raman bands of the surface vanadium oxide overlayer as well as weak bands of the $\delta, \theta\text{-Al}_2\text{O}_3$ support. The Raman bands of the support, however, quickly diminish as the vanadium oxide content is increased. This is due to the absorption of the laser light by the yellow-colored vanadium oxide overlayer. The Raman bands in the 990-1000 cm^{-1} region are characteristic of the distorted octahedra (decavanadate unit). The Raman bands in the 770-790, 530-540, and 150-300 cm^{-1} region are, however, much stronger than the corresponding Raman bands associated with the decavanadate ion and suggest the presence of a second

surface vanadium oxide species on the δ,θ - Al_2O_3 support. A similar set of Raman bands have recently been observed in a bismuth vanadate (Bi:V=25:1) reference compound which exhibits Raman bands at ~ 790 , 530 , 350 - 250 , and 150 cm^{-1} . Solid state ^{51}V NMR experiments have shown this structure to contain tetrahedral vanadium oxide species (15). The decrease in the Raman stretching frequency, from $\sim 830\text{ cm}^{-1}$ for monomeric VO_4^{3-} to $\sim 790\text{ cm}^{-1}$ for the bismuth vanadate (Bi:V=25:1), at the first approximation suggests, that the terminal V-O bonds have been slightly lengthened in this bismuth vanadate structure. Similar to the case of bismuth vanadium oxide compounds, the sodium vanadium oxide compounds ($\text{NaVO}_3 \rightarrow \text{Na:V}=1:1$; $\text{Na}_3\text{VO}_4 \rightarrow \text{Na:V}=3:1$) also show a decrease in Raman terminal stretching frequencies from ~ 920 to $\sim 820\text{ cm}^{-1}$ (16). Due to the presence of sodium ions on the surface, see Table I, it can be concluded that part of the surface vanadium oxide species are coordinated to surface sodium ions to form monomeric tetrahedral vanadia species. It is also possible to conclude that more than three sodium ions are coordinated per monomeric tetrahedral vanadium oxide species as the Raman band occurs below 820 cm^{-1} . Solid state ^{51}V NMR studies also confirm that two distinctly different surface vanadia species are present on the δ,θ - Al_2O_3 support: a perfect tetrahedral structure and a distorted octahedral structure (17). Thus, the supported vanadium oxide phase on δ,θ - Al_2O_3 consists of distorted octahedra (decavanadate-like) and monomeric tetrahedra.

The Raman spectra of supported vanadium oxide on α - Al_2O_3 exhibit different structural features than on the previously described alumina phases, as can be seen by comparing Figure 6 (0.7-1.7% $\text{V}_2\text{O}_5/\text{Al}_2\text{O}_3$) with Figures 4 and 5. Broad Raman features are present at ~ 770 , ~ 690 , ~ 550 , ~ 470 and a strong Raman band at $\sim 290\text{ cm}^{-1}$. As described previously, the $\sim 770\text{ cm}^{-1}$ band position is specific to the monomeric tetrahedral species with lengthened V-O bonds. It should be noted that the sodium ion concentration on the surface of α - Al_2O_3 is much higher than on other alumina supports (see Table I) and, hence, is most probably responsible for the formation of the monomeric tetrahedral species. Thus, the surface vanadium oxide phase on α - Al_2O_3 consists primarily of monomeric tetrahedral vanadia species. Similar spectra have been observed in our laboratory using different types of α - Al_2O_3 supports.

As mentioned earlier, sodium is usually present as an impurity in alumina. However, the absence of sodium on the surface of γ - Al_2O_3 implies its presence inside the bulk. To produce α and δ,θ - Al_2O_3 it is required to heat γ - Al_2O_3 to higher temperatures. As a result of heating γ - Al_2O_3 , sodium migrates to the surface. This can be observed in Table I where the sodium concentration increases from γ to α - Al_2O_3 . The migration of sodium changes the acid/base characteristics of the surface. An

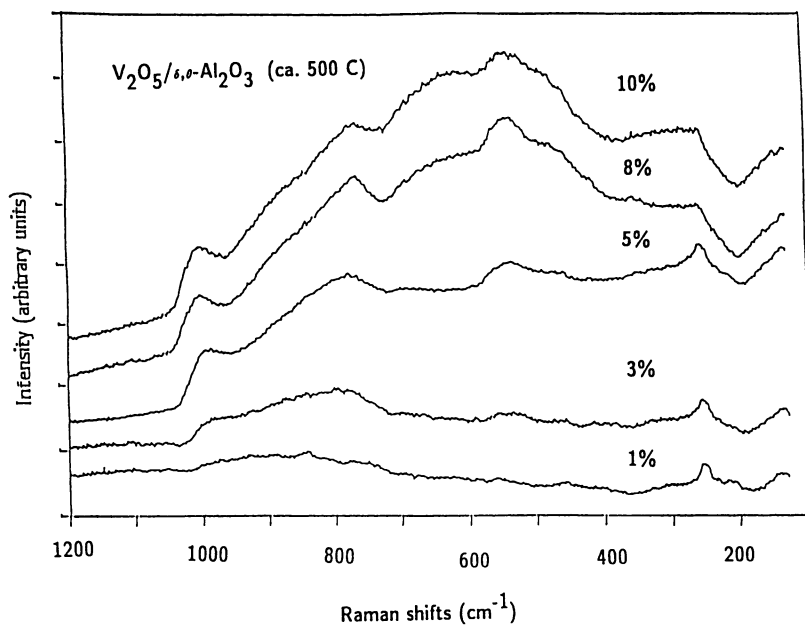


FIGURE 5. Raman Spectra of Vanadium Oxide Supported on $\delta,\theta-Al_2O_3$.

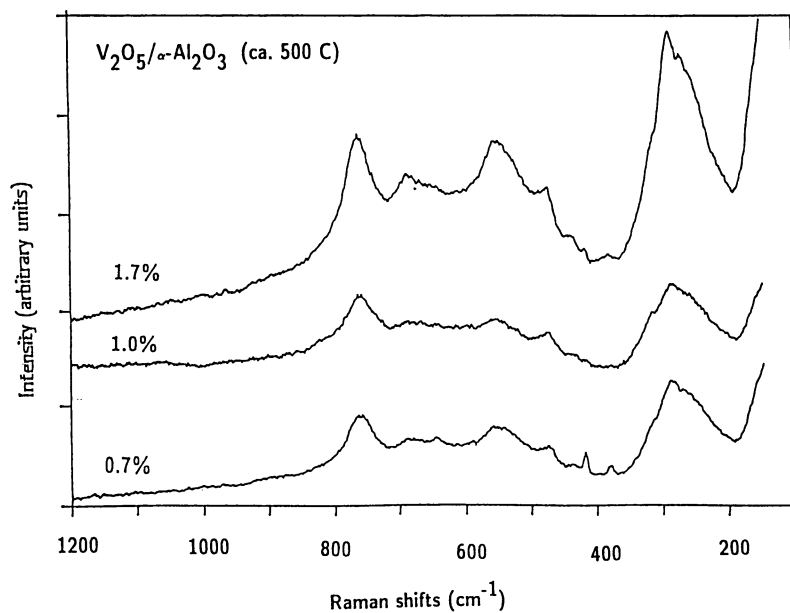


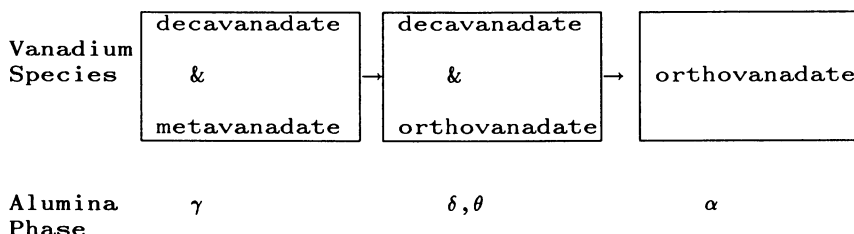
FIGURE 6. Raman Spectra of Vanadium Oxide Supported on $\alpha-Al_2O_3$.

increase in the sodium ion concentration produces a more basic surface. Thus, the basic strength of the surface should be expected to vary as follows:



← more basic

Comparison of this information with the surface vanadium oxide species present on the different alumina phases:



implies that acidic surfaces favor the decavanadate species, whereas, basic surfaces favor the orthovanadate species. Under ambient conditions, the conditions under which the $\text{V}_2\text{O}_5/\text{Al}_2\text{O}_3$ spectra were taken, the surface of the support is hydrated and there is a similarity in the behavior of the vanadium oxide surface species on Al_2O_3 and the pH dependence of aqueous vanadium oxide structural chemistry (10).

The effect of the impurities besides sodium do not seem to play an important role in determining the structure of the surface vanadium oxide species. Flourine is the only other impurity whose concentration varies appreciably in the different alumina phases. Flourine cannot be responsible for influencing the vanadium oxide structures since flourine is present in similar concentrations in α and $\delta,\theta\text{-Al}_2\text{O}_3$ while the vanadium oxide structures are changing. It may therefore be concluded that surface impurities other than sodium oxide do not contribute significantly to the change in the structure of the surface vanadium oxide species on the different alumina phases.

It should be noted that all of the above studies were performed under ambient conditions where the surface vanadium oxide species are known to be hydrated due to adsorbed moisture. It has been shown that dehydration can alter the structures of the surface vanadium oxide species. For example, dehydration of surface vanadium oxide species on $\gamma\text{-Al}_2\text{O}_3$, which initially possesses vanadia octahedra and tetrahedra, transforms most of the surface vanadia species to a tetrahedral coordination (4). Dehydration studies on the $\text{V}_2\text{O}_5/\delta,\theta\text{-Al}_2\text{O}_3$ and $\text{V}_2\text{O}_5/\alpha\text{-Al}_2\text{O}_3$ samples are currently underway.

CONCLUSIONS

The Raman spectra of model vanadium(V) oxide compounds are very sensitive to vanadium oxygen coordination. A distinct trend in the Raman spectra of the reference tetrahedral and octahedral vanadium(V) oxide compounds is observed. Vanadium oxide is found to interact differently with the different alumina supports. On the γ -Al₂O₃ support, the surface vanadium oxide overlayer consists of polymeric tetrahedra and distorted octahedra. On the δ, θ -Al₂O₃ support, the surface vanadium oxide overlayer is composed of monomeric tetrahedra and distorted octahedra. On the α -Al₂O₃ support, the surface vanadium oxide overlayer contains monomeric tetrahedra surface species. The interactions, however, appear to be primarily due to the level of sodium impurity present on the surface and not the alumina phase in particular. It is therefore imperative to take into consideration the surface impurities present when describing the molecular structures of the supported vanadium oxide phases.

ACKNOWLEDGMENTS

We would like to thank Jih-Mirn Jehng for obtaining the Raman spectra of some of the samples. This study has been supported by the National Science Foundation grant # CBT-8810714.

REFERENCES

- (a) F. Roozeboom, T. Fransen, P. Mars, and P. J. Gellings, *Z. anorg. allg. Chem.* 449, 25-40 (1979).
(b) F. Roozeboom, M. C. Mittelmeijer-Hazeleger, J. A. Moulijn, J. Medema, V. H. J. de Beer, and P. J. Gellings, *J. Phys. Chem.* 84, 2783 (1980).
(c) L. R. Le Coustumer, B. Taouk, M. Le Meur, E. Payen, M. Guelton, and J. Grimblot, *J. Phys. Chem.* 92, 1230 (1988).
- (a) R. Y. Saleh, I. E. Wachs, S. S. Chan, and C. C. Chersich, *J. Catal.* 98, 102 (1986). (b) I. E. Wachs, R. Y. Saleh, S. S. Chan, and C. C. Chersich, *Appl. Catal.* 15, 339 (1985).
- (a) J. Haber, A. Kozłowska, and R. Kozłowski, *J. Catal.* 102, 52 (1986). (b) H. Miyata, K. Fujii, T. Ono, and Y. Kubokawa, *J. Chem. Soc., Faraday Trans.* 1, 83, 675-685 (1987). (c) G. Bergeret, P. Gallezot, K. V. R. Chary, B. Rama Rao, and V. S. Subrahmanyam, *Appl. Catal.*, 40, 191 (1988). (d) J. Haber, A. Kozłowska, and R. Kozłowski, *Proc. 9th Intl. Congr. Catal.*, 1481-1488 (1988).
- (a) H. Eckert, and I. E. Wachs, *Mat. Res. Soc. Symp. Proc. Vol. 111*, 459 (1988). (b) H. Eckert, and I. E. Wachs, *J. Phys. Chem.*, 93, 6796 (1989)

5. I. E. Wachs, F. D. Hardcastle, S. S. Chan, Spectrosc., 1(8), 30 (1986).
6. W. P. Griffith, and P. J. B. Lesniak, J. Chem. Soc. A, 1066 (1969).
7. I. E. Wachs, and F. D. Hardcastle, Mat. Res. Soc. Symp. Proc., Vol. 111, 353 (1988).
8. H. Eckert, G. Deo, I. E. Wachs, and A. M. Hirt, J. of Colloids and Surfaces (in press).
9. I. E. Wachs, R. Y. Saleh, S. S. Chan, and C. C. Chersich, CHEMTECH, Dec., 756 (1985).
10. R. J. H. Clark, The Chemistry of Titanium and Vanadium, Elsevier Publishing Co., 1968.
11. J. M. Jehng, F. D. Hardcastle, and I. E. Wachs, Solid State Ionics, 32/33, 904 (1989).
12. H. T. Evans, Inorg. Chem., 5, 967-977 (1966).
13. H. N. Ng, and C. Calvo, Canad. J. Chem., 50, 3619-3624 (1972).
14. C. Misra, Industrial Alumina Chemicals, ACS monograph 184, 1986.
15. F. D. Hardcastle, I. E. Wachs, H. Eckert, and D. Jefferson, to be published.
16. F. D. Hardcastle and I. E. Wachs, to be published.
17. H. Eckert, G. Deo, and I. E. Wachs, to be published.

RECEIVED May 9, 1990